Dual-Port Output Control of Isolated DC/DC Converter Focusing on Duty Cycle and Frequency of Primary Inverter

Toshihiko Noguchi, Kazuki Shimizu, and Yoshinori Matsushita
Shizuoka University
noguchi.toshihiko@shizuoka.ac.jp, shimizu.kazuki.16@shizuoka.ac.jp

***Abstract*-This paper proposes a new approach of an isolated DC/DC converter with dual-port outputs. The converter has two outputs, i.e., a 12-V port and a 48-V port for automotive applications. The dual-port output control can independently be achieved by using only a single primary inverter and a single high-frequency transformer. The duty cycle and the frequency of the inverter are used to control the two output voltages at the same time. The both port voltages are regulated by means of manipulating the duty cycle and the frequency, respectively. In the paper, a technique to achieve the dual-port output voltage control of the isolated DC/DC converter is described and their control characteristics are investigated to confirm validity of the proposed technique.**

INTRODUCTION

As electric power consumption in a vehicle increases in recent years, the power supply voltage feeding to many kinds of the auxiliary equipment is changing from 12 V to 48 V. However, it is expected that the both voltages are redundantly used for a while because it is very hard to replace entire traditional 12-V components with 48-V components from the viewpoint of development cost; parts supply; maintenance service; market circumstances; and so forth. Therefore, a dual-port isolated DC/DC converter is demanded, which has capability to regulate two output voltages independently, and the total output power rating up to 2 kW is required for possibly increasing power consumption of a vehicle in the near future. The simplest scheme to create the both output ports is use of a non-isolated bidirectional buck-boost chopper. However, the chopper is inserted between the two output ports, so the cascade connection of power conversion makes the total efficiency worse. Using the two sets of the isolated DC/DC converter also has a drawback of high cost and large volume due to the increase of the electric devices such as MOSFETs, diodes, inductors, capacitors, etc.

In this paper, a novel technique to achieve the independent dual-port output control of the isolated DC/DC converter is proposed, which has only a single primary inverter and only a single high-frequency transformer. The proposed circuit features a series resonant circuit using as a variable impedance adjuster, and is based on the pulse width control (PWC) and the pulse frequency control (PFC) to achieve the independent control of the dual output ports. The paper describes the proposed circuit configuration and its operation principle, and clarifies the operation characteristics through some computer simulations, which proves feasibility of the proposed strategy.

CIRCUIT CONFIGURATION AND OPERATION OF PROPOSED DUAL-PORT DC/DC CONVERTER

A. *Circuit Configuration of Dual-Port DC/DC Converter*

The circuit configuration of the isolated dual-port DC/DC converter is shown in Fig. 1. The DC-bus voltage of the primary inverter is assumed to vary from 140 to 260 V, and the output frequency of the inverter is controlled around 400

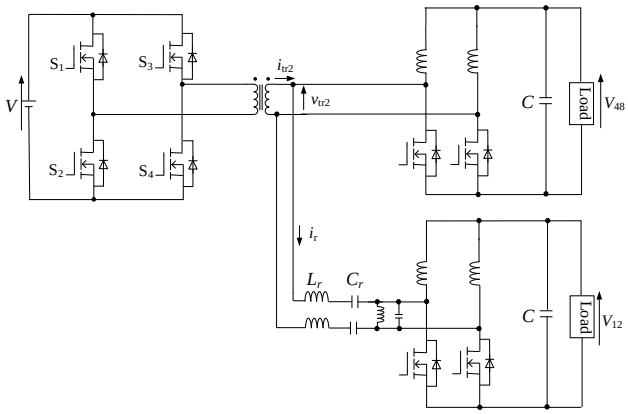

Fig. 1. Whole circuit configuration of isolated dual-port DC/DC converter.

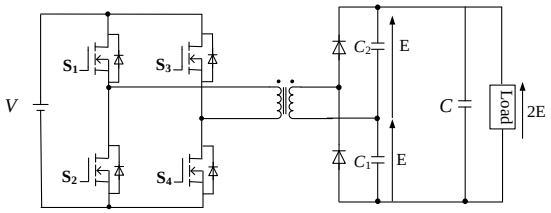

(a) Isolated DC/DC converter with voltage doubler.

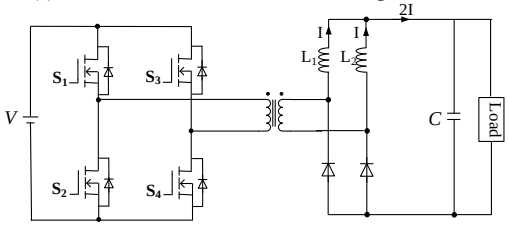

(b) Isolated DC/DC converter with current doubler.

Fig. 2. Classification of isolated DC/DC converters.

978-1-5090-2364-6/17/$31.00 ©2017 IEEE

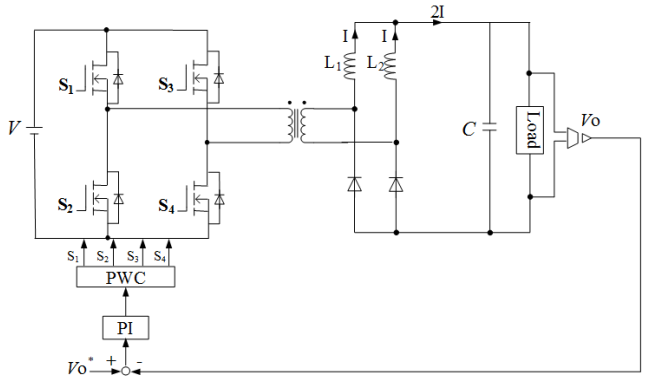

Fig. 3. Output voltage control of isolated DC/DC converter using PWC inverter.

kHz. The inverter has two degrees of freedom in controlling its output voltage, i.e., a duty cycle and a frequency of the output voltage pulse. In the proposed technique, the 48-V output port is controlled by using the duty cycle, which can be achieved with the PWC of the inverter. On the other hand, the 12-V output port is regulated by using the frequency, which can be controlled by the PFC of the inverter. Both of the secondary rectifying circuits of the 12-V and the 48-V output ports employ a double current topology because they have low-voltage and high-current output specifications. In addition, they introduce synchronous rectification using low-on-resistance MOSFETs to reduce their conduction losses.

B. Operation of Dual-Port DC/DC Converter

In general, power converters are classified into two categories; i.e., voltage-source converters and current-source converters. Fig. 2 shows the isolated DC/DC converters with the voltage-source or the current-source secondary rectifier. Fig. 2 (a) is a voltage doubling rectifier often used in a single-phase low-voltage AC/DC converter to boost the DC-bus voltage. Assuming the winding turn ratio of the high-frequency transformer is unity; a peak voltage E of the AC power source is applied across the capacitor C_1 through D_1 in a positive cycle, and is applied to C_2 through D_2 in a negative cycle. Therefore, the total DC-bus voltage is the summation of the voltages across the both capacitor $2E$. A dual circuit topology of the voltage doubler is a current doubler shown in Fig. 2 (b). When the inverter output is in a positive cycle, D_2 is turned on and the current I flows through the inductor L_1. This current I is held at a constant value while D_1 is turned on to make the current I flow into another inductor L_2 in a negative cycle of the inverter output. Therefore, the two currents flowing through L_1 and L_2 get together, and the total DC-bus current becomes $2I$.

Fig. 3 shows a block diagram of the output voltage control system, where the control error between the actual output voltage V_o and its command V_o^* is given to a PI regulator to determine the pulse width of the three-level inverter output voltage. The output voltage control loop makes the DC/DC converter robust against variations of the power source voltage and the load power.

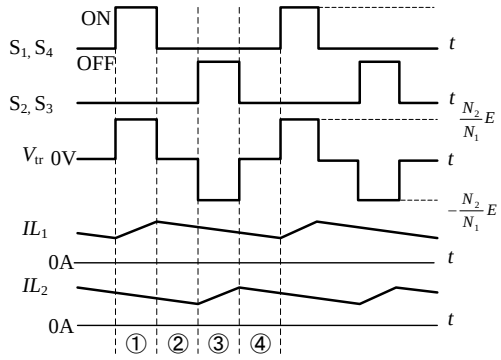

Fig. 4. Operation waveforms of isolated DC/DC converter with current doubler rectifier in secondary circuit.

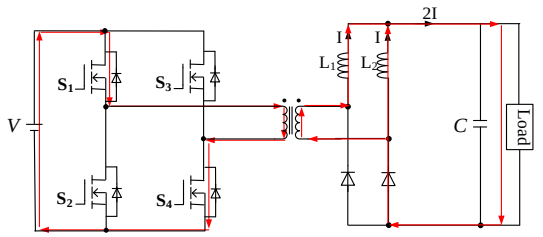

(a) Positive cycle (L_1 charged and L_2 discharged).

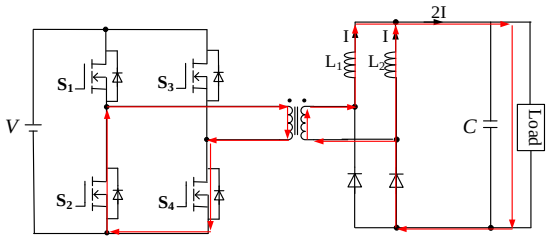

(b) Current holding period (both L_1 and L_2 discharged).

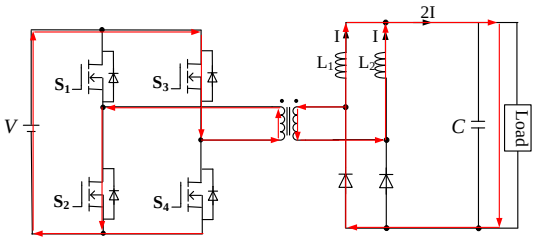

(c) Negative cycle (L_1 discharged and L_2 charged).

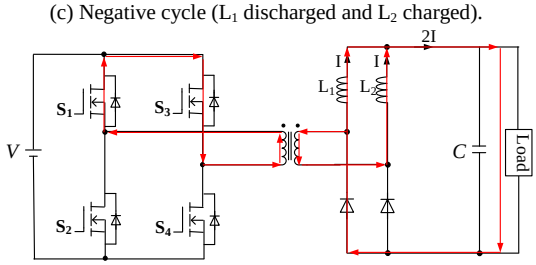

(d) Current holding period (both L_1 and L_2 discharged).

Fig. 5. Circuit operation modes of isolated DC/DC converter with current doubler in secondary circuit.

Fig. 4 illustrates operating waveforms of the isolated DC/DC converter with the current doubler, where the circuit operation is divided into four modes indicated in Fig. 5. The primary inverter outputs the three-level voltage waveform, whose pulse width is determined by the PWC. The transformer is excited in the positive direction in the mode (a),

where the diode D_1 is off and D_2 is turned on. Therefore, the current $2I$ having flown into the diode D_2 is shunted to L_1 and L_2. Since the energy is stored in L_1 in the mode, the current flowing into L_1 gradually increases, while the current of L_2 decreases because its stored energy is released to the load. The output voltage of the inverter becomes zero in the next mode (b), so the current $2I$ flowing into D_2 diverges to L_1 and L_2 with decreasing the amplitudes and the energies of the both. The operation mode (c) is the inverse of the mode (a), and L_1 stores its energy and L_2 releases its energy to the load because D_1 is turned on and D_2 is turned off. Hence, the current flowing into L_1 increases and the current of L_2 gradually decreases. The operation mode (d) is basically same as the mode (b).

Assuming that the total resistnce of the MOSFETs and the inductors on the secondary side is R and that the load current is I, the power loss of the current doubler is calculated as

$$P_{loss} = 2R\left(\frac{I}{2}\right)^2 = \frac{R}{2}I^2 \quad . \tag{1}$$

Therefore, it is possible to halve the power loss by using the current doubling rectifier, which is significantly effective for low-voltage and high-current applications.

C. Dual-Port Output Control with PWC and PFC

The 48-V output port of the proposed DC/DC converter is regulated by means of the PWC, while the 12-V output port is done by the PFC. Since the secondary rectifier employs a current doubling synchronous rectifying technique to reduce the conduction loss, the steady state output voltage of the 48-V port V_{48} is controlled by the duty cycle D as follows:

$$V_{48} = \frac{DV}{2a}, \tag{2}$$

where V represents the DC-bus voltage of the primary inverter and a is the winding turn ratio of the high-frequency transformer. Because the primary side is constituted with a full-bridge inverter, the adjustable range of D is $0 \le D \le 0.5$ as shown in Fig. 6.

As for the 12-V output port, a series and parallel resonant circuits are inserted in front of the secondary rectifier. The parallel resonant circuit is inserted for the purpose of decoupling the series resonant circuit from the inductors of the current doubler. The output voltage of the 12-V port V_{12} is controlled by manipulating an impedance of the series resonant circuit with respect to the inverter output frequency. The impedance of the series resonant circuit Z_r can be expressed as

$$Z_r = \sqrt{R_r^{\,2} + \left(\frac{\omega^2 L_r C_r - 1}{\omega C_r}\right)^2}, \tag{3}$$

where L_r, C_r, and R_r are an inductance, a capacitance, and a resistance of the series resonant circuit, respectively. Fig. 7 is the impedance characteristic with respect to the frequency, assuming that the inductance and the capacitance values are same as those used in the computer simulations and R_r = 10 Ω. It is confirmed that the impedance is the minimum at the point of the resonant frequency and that the impedance can be

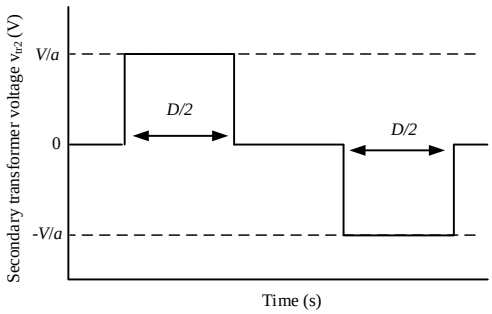

Fig. 6. Secondary voltage waveform of high-frequency transformer.

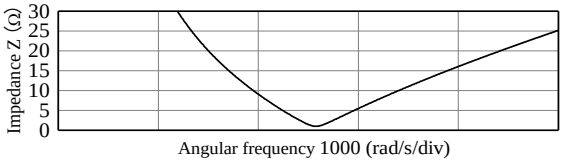

Fig. 7. Impedance characteristic of resonant circuit.

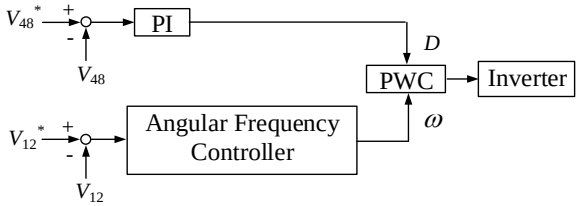

Fig. 8. Block diagram of dual-port voltage controller.

controlled by manipulating the frequency. The output voltage of the 12-V port V_{12} is expressed as the following equation;

$$V_{12} = \frac{DVZ}{2a(Z_r + Z)}, \tag{4}$$

where the total impedance of the load and the smoothing capacitor across the 12-V output port is Z and the parallel resonant circuit is assumed to be ideal.

It is found from (2) and (4) that V_{48} can be controlled by D and that V_{12} can be done by D and ω. Because 48-V output voltage control is independent of the frequency ω, the both output voltages are controllable by manipulating D and ω at the same time. Fig. 8 shows a block diagram of the controller described above.

D. Soft Switching Operation of Primary Inverter

It is possible to utilize a soft switching technique owing to the resonant current in the primary inverter caused by the series resonant circuit. The primary current includes not only the resonant current but also the current of the current doubling rectifier. A condition to achieve the soft switching is to make the current lagging. In other words, it is required to make the frequency higher than the resonant frequency, resulting in a zero-current switching (ZCS) during turning on of the switching devices. On the other hand, a zero-voltage switching (ZVS) during turn off process is possible by connecting capacitors to the switching devices in parallel. These soft switching techniques possibly reduce the switching losses and EMI/EMC noises because they restrict the d*v*/dt and/or d*i*/dt.

TABLE I. SIMULATION PARAMETERS.

Parameters	Values
DC-bus voltage	200 V
Resonance frequency	410 kHz
48-V port output power	1 kW
12-V port output power	1 kW
Turn ratio of transformer	7:4
Resonant inductor	6.8 μH
Resonant capacitor	22 nF
48-V port smoothing capacitor	4.7 μF
12-V port smoothing capacitor	10 μF
48-V port inductor	10 μH
12-V port inductor	5 μH

VERIFICATION OF CIRCUIT OPERATION THROUGH COMPUTER SIMULATIONS

A. Control Characteristics in Steady State

Computer simulations have been conducted to examine the control characteristics of the isolated DC/DC converter based on the proposed strategy. Various parameters used in the simulations are listed in TABLE I. As the frequency response of the resonant circuit impedance has a steep characteristic, the primary inverter is operated in the lower-frequency range than the resonant frequency. This implies that the adjustable range of the operating frequency can be narrow to control the output port V_{12} although the soft switching technique cannot be applied. It is assumed that the load power of the both output ports is 1 kW; hence, the 48-V output port current and the 12-V output port current are 20.8 A and 83.3 A, respectively.

Figs. 9 and 10 show the simulation results of the operating waveforms under the above condition. From the top to the bottom, the 48-V output port V_{48}, the 12-V output port V_{12}, the secondary current of the transformer i_{tr2}, the secondary voltage of the transformer v_{tr2}, and the series resonant circuit current i_r are indicated in the figures. It is confirmed from Fig. 9 that the voltages V_{48} and V_{12} of the both output ports are stably regulated at their command values for the long period. Fig. 10 is expanded waveforms. As can be seen in the figure, the output voltages V_{48} and V_{12} are following their commands with small tolerance, and their ripple frequencies are double of the primary inverter output frequency. There is a phase difference between the secondary current and the secondary voltage of the transformer, which is caused by the inverter operating frequency lower than the resonant frequency. Since the 12-V output port is controlled by means of the PFC as described previously, the phase difference is dependent of the load power of the 12-V output port. The operating frequency range determined by the PFC must be restricted because the low-operating-frequency causes magnetic saturation in the transformer and the inductors of the current doublers. Therefore, the operating frequency range is limited within $\pm 250 \times 10^3$ rad/s.

Fig. 11 (a) shows static load regulation characteristics of the isolated dual-port DC/DC converter. The graph lines with

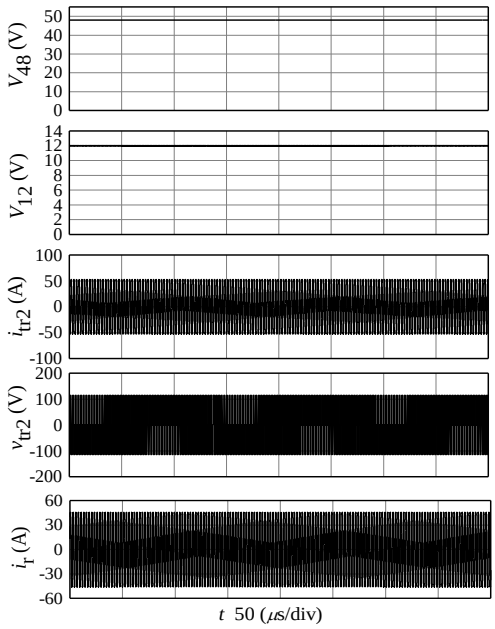

Fig. 9. Operating waveforms of isolated dual-port DC/DC converter.

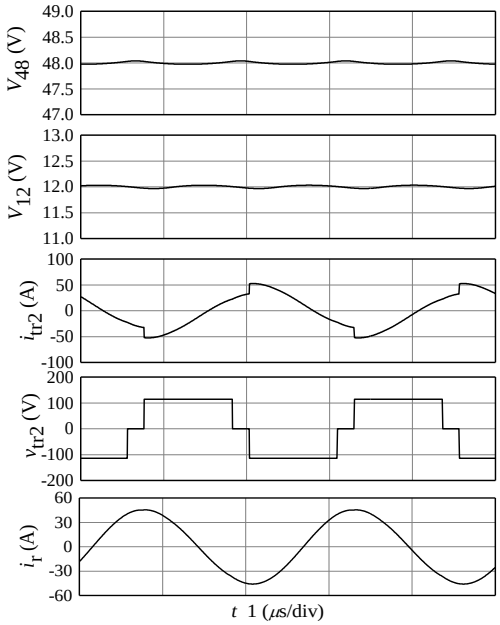

Fig. 10. Expanded operating waveforms.

square symbols are average voltages of the 48-V output port with respect to the load power under a 100-% fixed load condition of the 12-V output port. The other graph lines with circle symbols are the 48-V characteristics under the condition of a 10-% fixed load on the 12-V output port. In the similar way, the triangle symbols represent the 12-V characteristics with a 100-% fixed load condition on the 48-V output port, while the inversed triangle symbols are the 12-V characteristics with keeping 48-V port load at 10 %. As can be seen in the figure, both of the output port voltages are controlled properly at 48 V and 12 V regardless of the load power variation. In addition, independent load regulation characteristics can be confirmed between the two output ports.

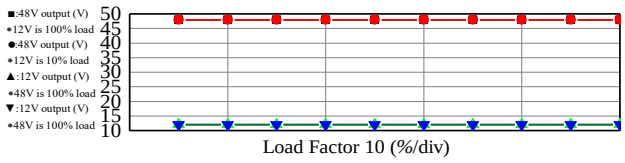

(a) Steady-state output voltage characteristics to load variations.

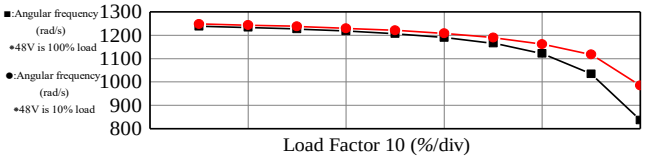

(b) Relationship between load power and operating frequency.

Fig. 11. Load regulation characteristics.

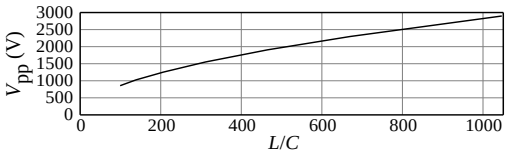

Fig. 12. Voltage across capacitance in resonant circuit.

Fig. 11 (b) shows relationships between the operating frequency and the load power. Every symbol stands for the same operating condition as described in Fig. 11 (a). It is inferred that the frequency variation is remarkably large in the heavy load range of the 48-V output port because the current flowing into the parallel resonant circuit is reduced and is hard to damp in the heavy load range. When the load power of the 12-V output port is low, the operating frequency also decreases because the quality factor of the series resonant circuit becomes low. Therefore, it is rather difficult to operate the 12-V output port under condition less than 10-% load power, which may require a dummy load sacrificing the efficiency in the light load range.

It is definitely necessary to design the resonant circuit so that the resonant characteristic has an appropriate quality factor. If the impedance characteristic with respect to the frequency is too steep, even a small frequency change may cause a large output voltage variation. In order to make the PFC stable, therefore, the quality factor of the resonant circuit should not be too high. The voltage characteristic in the resonant circuit is shown in Fig. 12, where the quality factor of the resonant circuit is changed. The actual voltage is lower than the characteristic shown in the figure because the resistive component is ignored in the resonant circuit. It is found that the quality factor must be determined from the viewpoint of withstanding voltages of the resonant inductors and the resonant capacitors, too.

B. Dynamic Response to Disturbance Load

Disturbance load tests have been conducted through the simulations to confirm the dynamic responses of the proposed DC/DC converter. From the top to the bottom in Fig. 13, the step disturbance response of the 48-V output port is indicated under a condition of 100-% continuous load power on the 12-V output port. The load of the 48-V output port has been changed stepwise from 20 % to 100 % and vice versa. The

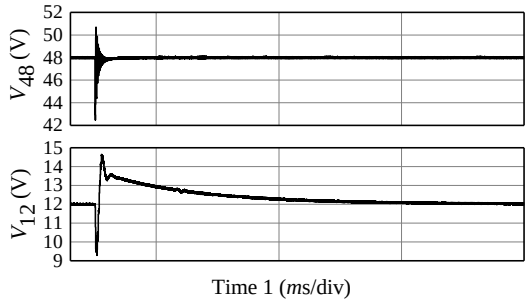

(a) Step disturbance response of 48-V output port from 20 % to 100 %.

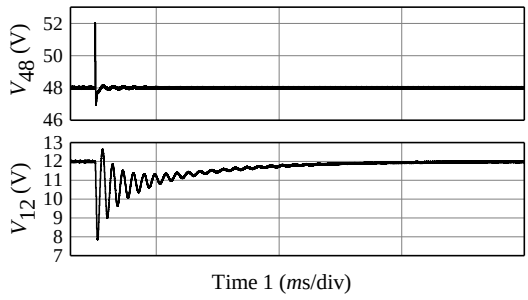

(b) Step disturbance response of 48-V output port from 100 % to 20 %.

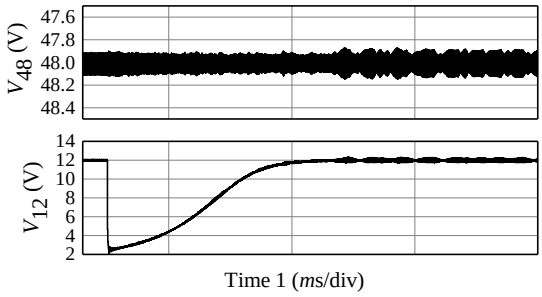

(c) Step disturbance response of 12-V output port from 20 % to 100 %.

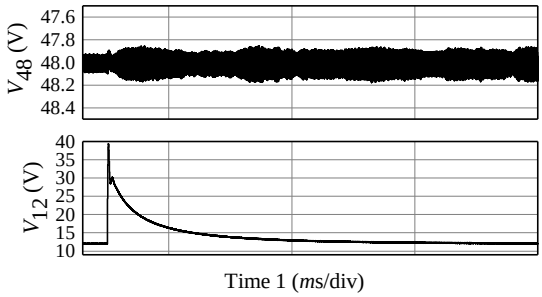

(d) Step disturbance response of 12-V output port from 100 % to 20 %.

Fig. 12. Step disturbance responses of isolated dual-port DC/DC converter.

second waveforms show the step disturbance response of the 12-V output port with continuously making the 48-V output port load 100 %. Although the convergence time back to the command voltages 48 V and 12 V takes approximately 2 ms, both of the output port voltages asymptotically return to the command values. As (2) and (4) indicate, D starts to change when the disturbance is applied to the 48-V output port, resulting in the time variations of the both output port voltages. However, 48-V output port is not affected by the disturbance to the 12-V output port because 48-V output port is controlled by only D and has nothing to do with the frequency. Since the resonant circuit is employed in the 12-V circuit, the dynamic behavior of V_{12} is much slower than that

of V_{48}, which is caused by a high-quality-factor design of the resonant circuit. Therefore, the resonant current is hard to change owing to the high-quality-factor, and it takes a long time for the command value to be effective to the DC/DC converter, resulting in the long convergence tine. This problem van be solved by reducing the quality factor, but the volumes of the transformer and the inductors may be large because the variation range of the frequency is wider due to the low-quality-factor design. It is necessary to choose the appropriate quality factor of the resonant circuit by taking the withstanding voltage of the components, frequency variation range, and disturbance response into account.

CONCLUSION

In this paper, a dual-port output control strategy of the isolated DC/DC converter has been discussed, which is capable to regulate the two output voltages simultaneously and independently. The control is achieved by manipulating the duty cycle and the frequency of the high-frequency PWC inverter. It has been confirmed through several computer simulations that the both output voltages are controlled accurately and independently even if the step load change is applied to one port, which proves feasibility of the proposed strategy.

REFERENCES

[1] Y. Chan, Y. Matsushita, T. Noguchi, O. Kimura, and T. Sunayama, "Current Boost DC/DC Converter Using Multi-Phase Inverter," *Proceedings of IEEJ Industry Applications Society Annual Conference*, vol. 1, 2015, pp. 353-356.

[2] T. Teratani, "Impact of DC48V on Automotive Power Supply System," *IEEJ Transactions on Industry Applications*, vol. 135, no. 9, pp. 892-897.

[3] M. Ishigaki, K. Ito, N. Yanagisawa, S. Tomura, and T. Umeno, "Novel of Isolated Multi-Port Converter for Integrating Complex DC Power Systems," *IEEJ Transaction on Industry Applications*, vol. 134, no.10, pp. 844-852.

[4] C. Zhao, S. D. Round, and J. W. Kolar, "An Isolated Three-Port Bidirectional DC-DC Converter with Decoupled Power Flow Management," *IEEE Transactions on Power Electronics*, vol. 23, no. 5, 2008, pp. 2443-2453.

[5] T. G. Wilson, "The Evolution of Power Electronics," *IEEE Transactions on Power Electronics*, vol. 15, no. 3, 2000, pp. 439-446.

[6] J. P. Barton and D. G. Infield, "Energy Storage and Its Use with Intermittent Renewable Energy," *IEEE Transactions on Power Electronics*, vol. 19, no. 6, 2004, pp. 441-448.

[7] F. Caricchi, F. Crescimbini, O. Honorati, and E. Santini, "Testing of a New DC/DC Converter Topology for Integrated Wind-Photovoltaic Generating Systems," *Proceeding of IEEE Power Electronics and Applications Conference*, vol. 8, 1993, pp. 83-88.

[8] L. Solero and F. Crescimbini, "Performance of a 10 kW Power Electric Interface for Combined Wind/PV Isolated Generating Systems," *IEEE Transactions on Industry Applications*, vol. 38, no. 4, 1996, pp. 1027-1032.

[9] Y. M. Chen, Y. C. Liu, and F, Y. Wu, "Multi-Input DC/DC Converter Based on the Multiwinding Transformer for Renewable Energy Applications," *IEEE Transactions on Industry Applications*, vol. 38, no. 4, 2002, pp. 1096-1104.

[10] Z. Chen and Y. Hu, "A Hybrid Generation System Using Variable Speed Wind Turbines and Diesel Units," *Proceeding of IEEE Industrial Electronics Conference*, vol. 3, 2003, pp. 2729-2734.

[11] K. Strunz and E. K. Brock, "Hybrid Plant of Renewable Stochastic Source and Multilevel Storage for Emission-Free Deterministic Power Generation," *Proceeding of International Symposium on Quality and Security of Electric Power Delivery Systems*, 2003, pp. 214-218.

[12] D. Das, R. Esmaili, L. Xu, and D. Nichols, "An Optimal Design of a Grid Connected Hybrid Wind/Photovoltaic/Fuel Cell System for Distributed Energy Production," *Proceeding of IEEE Transactions on Industrial Electronics Conference*, 2005, pp. 2499-2504.

[13] K. Kobayashi, H. Matsuo, and Y. Sekine, "Novel Solar-Cell Power Supply System Using a Multiple-Input DC-DC Converter," *IEEE Transactions on Industrial Electronics*, vol. 53, no. 1, 2006, pp. 281-286.

[14] Y. M. Chen, C. S. Cheng and H. C, Wu, "Grid-Connected Hybrid PV/Wind Power Generation System with Improved DC Bus Voltage Regulation Strategy," *Proceeding of IEEE Applied Power Electronics Conference*, 2006, pp. 1088-1094.

[15] H. Tao, J. L. Duarte, and M. A. Hendrix, "Multiport Converter for Hybrid Power Sources," *Proceeding of IEEE Power Electronics conference*, 2008, pp. 3412-3418.

[16] R. Jayabalan and B. Fahimi, "Monitoring and Fault Diagnosis of Multi-Converter Systems in Hybrid Electric Vehicles," *IEEE Transactions on Vehicular Technology*, vol. 55, no. 5, 2006, pp. 1475-1484.

[17] J. Y. Lee, Y. M. Chang, and F. Y. Liu, "A New UPS Topology Employing a PFC Boost Rectifier Cascaded High-Frequency Tri-Port Converter," *IEEE Transactions on Industrial Electronics*, vol. 46, no. 4, 1999, pp. 803-813.

[18] H. Pinheriro and P. K. Jain, "Series-Parallel Resonant UPS with Capacitive Output DC Bus Filter for Powering HFC Networks," *IEEE Transactions on Power Electronics*, vol. 17, no. 6, 2002, pp. 971-979.

[19] F. D. Rodriguez and W. G. Imes, "Analysis and Modeling of a Two-Input DC/DC Converter with Two Controlled Variables and Four Switched Networks," *Proceeding of Intersociety Energy Conversion Engineering Conference*, vol. 1, 1996, pp. 322-327.

[20] J. Sebastian, P. J. Villegas, F. Nuno, and M. M. Hernando, "High-Efficiency and Wide-Bandwidth Performance Obtainable from a Two-Input Buck Converter," *IEEE Transactions on Power Electronics*, vol. 13, no. 4, 1998, pp. 706-717.